Inhibition of the Serotonin 5-HT_3 Receptor by Nicotine, Cocaine, and Fluoxetine Investigated by Rapid Chemical Kinetic Techniques†

Hans-Georg A. Breitinger,‡ Natarajan Geetha,§ and George P. Hess*

Department of Molecular Biology and Genetics, 216 Biotechnology Building, Cornell University, Ithaca, New York 14853-2703

Received April 5, 2001

ABSTRACT: The 5-HT_3 serotonin receptor plays an important role in regulating communication between cells in the central and peripheral nervous systems. It is the target of many different therapeutic agents and abused drugs. A rapid chemical kinetic method with a time resolution of 10 ms in combination with the whole-cell current-recording technique was employed to study the receptor in NIE-115 mouse neuroblastoma cells. The mechanism of the channel-opening process, receptor desensitization, and receptor inhibition by nicotine, cocaine, and fluoxetine were investigated. Two different forms of the 5-HT_3 serotonin receptor, each with a different desensitization rate, were observed. The inhibition of the receptor by nicotine has not previously been reported. Both nicotine and cocaine compete with serotonin for the receptor site that controls channel opening, with observed dissociation constants of 25 and 7 μM, respectively. Fluoxetine (Prozac), a widely used antidepressant, occupies a different regulatory site on the receptor with an apparent K_i value of 244 μM.

Rapid chemical kinetic techniques with a time resolution of 10 ms were used to investigate the mechanism of channel opening of the serotonin type 3 (5-HT_3) receptor on NIE-115 mouse neuroblastoma cells (*1*), the receptor desensitization reaction, and the mechanism of receptor inhibition by nicotine, cocaine, and fluoxetine. These inhibitors were chosen because the actions of both nicotine and cocaine on the nervous system are of major concern to society worldwide (*2*). Fluoxetine (Prozac) is an important therapeutic agent and commonly used antidepressant (*3*).

Like the nicotinic acetylcholine and glutamate receptors, the 5-HT_3 serotonin receptor is an excitatory, cation-conducting ligand-gated ion channel. It is the only known ligand-gated ion channel in the serotonin receptor family (*4*, *5*). To date only a few chemical kinetic investigations of the receptor have been reported. Yakel and colleagues (*6*) reported that desensitization of the 5-HT_3 receptor in NG 108-15 cells is regulated by two or more complex processes with varying requirements for ATP hydrolysis. A double-exponential time course for desensitization was reported by Yakel (*7*) for homomeric 5-HT_3 receptor channels expressed in *Xenopus* oocytes. It has been reported that cocaine and fluoxetine inhibit the 5-HT_3 receptor expressed in *Xenopus laevis* oocytes (*8*) and rat nodose ganglia (*9*), respectively. The mechanism of activation of the 5-HT_3 receptor and its inhibition by cocaine and fluoxetine are not well understood, nor has inhibition of the receptor by nicotine been reported previously. Investigation of the mechanism of receptor activation and inhibition was the objective of this study.

MATERIALS AND METHODS

Cell Culture and Maintenance. NIE-115 cells (*1*) were grown in 80 cm^2, 260 mL Nunc culture flasks (Krackeler Scientific, Albany, NY) at a temperature of 37 °C in a water-saturated atmosphere containing 5% CO_2. Twenty-five milliliters of culture medium per flask made up of Dulbecco's modified Eagle's medium (DMEM, low glucose, GibcoBRL, Grand Island, NY) supplemented with 8% fetal bovine serum (FBS, GibcoBRL) were used. Antibiotics (100 IU of penicillin, 100 μg/L streptomycin, both from Sigma, St. Louis, MO) were added to the medium only if contamination was observed. Cells were transferred weekly, seeded at 5×10^5 cells/flask, and fed twice during that period by replacing half of the old medium with fresh medium. On the day of transfer, cells were plated into 35 mm Falcon dishes (2 mL of cell suspension of 1×10^4 cells/mL per dish). These cells were then used for experiments within 2−5 days.

Whole-Cell Recording. Recording glass electrodes were pulled from borosilicate glass (World Precision Instruments Inc., Sarasota, FL), using a two-stage puller (L/M 3 P-A, Adams & List, New York, NY) and a flame polisher (MF-83, Narishige, Tokyo, Japan). The extracellular buffer contained 125 mM NaCl, 5.5 mM KCl, 1.8 mM $CaCl_2$, 0.8 mM $MgCl_2$, 24.0 mM glucose, 37.0 mM sucrose, and 20 mM HEPES; the pH was adjusted to 7.2 with NaOH. The electrode solution contained 150 mM KCl, 10 mM NaCl, 1.0 mM $MgCl_2$, and 10.0 mM HEPES; the pH was adjusted to 7.2 with KOH (composition of both buffers according to H. P. M. Vijverberg, private communication). An Axopatch 200A amplifier (Axon Instruments, Foster City, CA) was used for recordings. Signals were acquired using the pClamp software packet (Axon Instruments). Data were analyzed off-line on a PC using Microcal Origin software (Microcal,

† This work was supported by a postdoctoral fellowship awarded to H.-G.A.B. by the Swiss Academy of Sciences, and by National Institutes of Health Grant DA11643 awarded to Robert E. Oswald and G.P.H.

* Address correspondence to this author. Tel: (607) 255-4809; FAX: (607) 255-6249; email: gph2@cornell.edu.

‡ Present address: University of Erlangen-Nuremberg, Institute for Biochemistry, Fahrstrasse 17, D-91054 Erlangen, Germany.

§ Present address: Department of Chemistry, Palomar College, San Marcos, CA 92069.

10.1021/bi0106890 CCC: $20.00
Published on Web 06/19/2001

Northampton, MA). All measurements were carried out at pH 7.2, 21−23 °C, at a transmembrane voltage of −60 mV. Data from each cell were normalized to the response measured with 10 μM serotonin. All solutions used in the experiments were prepared on the day of measurements. Serotonin (1 mM), nicotine (10 mM), and fluoxetine (1 mM) stock solutions could be stored at −20 °C for several weeks. The cocaine stock solution (1 mM) was prepared on the day of measurement from the hydrochloride. All other chemicals were obtained from commercial sources; the creatinine sulfate complex of serotonin was obtained from Sigma.

Rapid Application of Ligand Solution. The flow method used for rapid ligand application has been described elsewhere (*10, 11*). In brief, a cell (ca. 30−50 μm diameter) in the whole-cell recording configuration (*12*) was placed at a distance of ca. 100 μm from the porthole (diameter ca. 100 μm) of a U-tube (*10*) which was made from stainless-steel HPLC tubing (Hamilton, Reno, NV). The flow rate of solutions emerging from the flow device, containing neurotransmitter without and with inhibitor, was typically ∼1 cm/s. With 10 μM serotonin, the observed rise time of the whole-cell current to its maximum value, characteristic of the time for serotonin to equilibrate with the cell surface receptors, was 80−100 ms; receptor desensitization during this time can be significant. The current is, therefore, corrected for desensitization in our experiments as described previously using eq 1 (Appendix) (*11, 13*). If a fraction of current remained after the desensitization reaction had gone to completion (usually less than 5% of the total current), it was subtracted from the observed current before correction. Cells were allowed to recover for 2 min between each experiment, a time sufficient to guarantee full resensitization of the receptors (*14*).

RESULTS

A minimum reaction scheme (Appendix), which requires the binding of two neurotransmitter molecules to the receptor before the channel opens followed by a slow (seconds time region) receptor desensitization, was first suggested by Katz and Thesleff for the acetylcholine receptor (*15*). The minimum reaction Scheme 1 (Appendix) shows only the fast desensitization process (millisecond time region) first discovered in chemical kinetic investigations of the acetylcholine receptor (*16, 17*). This precedes a slow process first reported in investigations of the acetylcholine receptor by Katz and Thesleff, using classical electrophysiological techniques (*15*). Reaction Scheme 1 has been shown to account for acetylcholine receptor-mediated reactions in the *Electrophorus electricus* electric organ (*16, 17*), and BC_3-H1 muscle cells (*11, 18*), as well as for the action of $GABA_A$ (*19*) and glycine (*20*) receptors in central nervous system neurons. It also underlies the inhibition of the acetylcholine receptor in BC_3H1 cells by procaine (*21*) and cocaine (*22*). Here we show that this reaction scheme also satisfactorily describes the concentration dependence of serotonin-evoked currents in NIE-115 cells containing 5-HT_3 receptors.

Figure 1A shows a whole-cell current measurement made in the presence of 10 μM serotonin with a NIE-115 mouse neuroblastoma cell, using the cell-flow technique (*11, 13*). The current (solid line) reaches a maximum within 100 ms. Two exponentials plus a constant term are needed to fit the decaying phase of the current, which is considered to reflect receptor desensitization. In the experiment shown in Figure 1A, the rate coefficients for receptor desensitization, α and β, had values of 7.3 and 0.3 s^{-1}, respectively. The current corrected for desensitization that occurs during the equilibration of the neurotransmitter with the cell surface receptors is shown by the dashed line, which was calculated using eq 1 (Appendix) (*11, 13*). In this experiment, the ratio of the current amplitudes corrected for receptor desensitization associated with the rapidly and slowly decaying phases of the current, I_α/I_β, is 2.3. If the falling phases of the current observed in two time regions reflected two consecutive desensitization processes, or two parallel desensitization reactions involving the undesensitized receptor, the ratio of I_α/I_β would be expected to remain constant at a constant concentration of serotonin. In 30 experiments with 30 different cells, which exhibited 2 different desensitization processes at serotonin concentrations ranging from 2 to 100 μM, the ratio I_α/I_β was found to vary significantly between different cells when measurements at the same serotonin concentration were compared (Table 1). The results in Table 1 indicate that the NIE-115 cells contain two different receptor forms that do not interconvert on the time scale of the experiments. Similar results indicating the presence of two receptor forms have been obtained with the γ-aminobutyric acid ($GABA_A$) receptor in rat brain membrane vesicles (*23*) and mouse cortical cells (*19*) and with the glycine receptor in mouse spinal cord cells (*20*). We were also able to identify NIE-115 cells that exhibited only the slower of the two desensitization processes (see below).

Table 1: Effect of Serotonin Concentration on the Ratio of the Maximum Current Amplitudes Corrected for Receptor Desensitization, I_α/I_β, Associated with the Rapid and Slow Phases of Receptor Desensitization[a]

[serotonin] (μM)	no. of cells	I_α/I_β
100	6	0.30, 0.35, 0.35, 0.39, 1.28, 1.31, 1.47
10	11	0.37, 0.40, 0.40, 0.56, 0.60, 0.86, 0.94, 1.72, 2.04, 4.50, 7.31
50	8	0.28, 0.40, 0.96, 1.18, 1.23, 1.25, 1.38, 2.22
3	2	0.51, 0.69
2	2	0.45, 0.70

[a] Measurements were carried out at 21−23 °C, pH 7.2, and a transmembrane voltage of −60 mV.

Figure 1B shows the dependence of the concentration of open receptor-channels on serotonin concentration. The squares represent data that were obtained with cells where the observed desensitization of the whole-cell current could satisfactorily be described as a single-exponential process. The desensitization rate coefficient (1.5−0.1 s^{-1}) in the range of serotonin concentration used indicates that we were observing the slowly desensitizing receptor form. The open symbols represent data obtained from cells that showed a two-exponential time course of desensitization. The total current (the sum of both the slow and the fast desensitizing phase, I_α and I_β) is represented by the open symbols in Figure 1B. For all subsequent analyses, only data that showed a single-exponential desensitization process were used. A nonlinear fit of these data to eq 2 (Appendix) gave the solid line. The values of the constants accounting for the observed

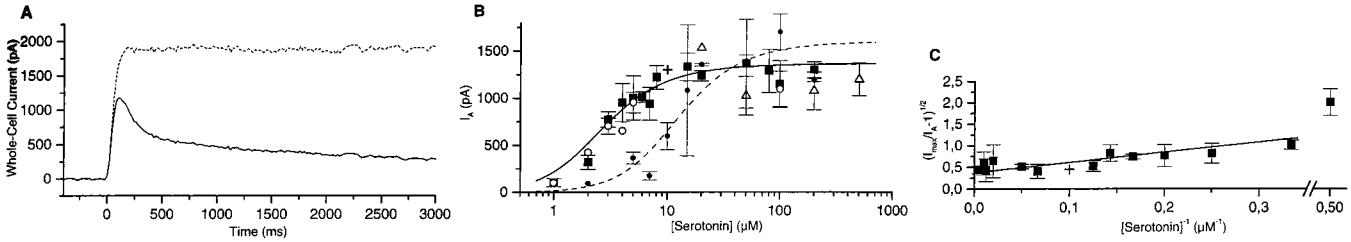

FIGURE 1: Cell-flow investigations of the effects of serotonin and nicotine on 5-HT$_3$ receptors of NIE-115 mouse neuroblastoma cells. (A) Whole-cell current response of the receptors to 10 μM serotonin. All measurements were carried out at pH 7.2, 21−23 °C, $V_m = -60$ mV, using a cell-flow technique (*10, 11*) and a flow rate of the serotonin solution of ∼1 cm/s for the rapid equilibration of cell surface receptor with the ligand. The observed whole-cell current (solid line) is a measure of the number of receptors in the open-channel form in the cell membrane and reaches a maximum value in ∼100 ms. The falling phase of the current, indicative of receptor desensitization, reveals two processes: ∼70% of the current decays with a rate coefficient of 7.3 s^{-1}, and ∼30% of the current decays with a rate coefficient of 0.3 s^{-1}. A small fraction of the current (∼5%) does not decay during 10 s of observation. The broken line that becomes parallel to the time axis represents the current corrected for desensitization that occurs during the rising phase of the current (*11*; eq 1). (B) Dependence of the whole-cell current on the concentration of serotonin. I_A is the current amplitude obtained in cell-flow experiments (*11*), corrected for receptor desensitization (see panel A). Measurements were made at pH 7.2, 21−23 °C, $V_m = -60$ mV. (+) Normalization point at 10 μM serotonin, 1300 pA. The average response from cells used for evaluation to the application of 10 μM serotonin was used to calculate the normalization current value. The current obtained with the 27 cells used in the experiments in the presence of 10 μM serotonin ranged from 500 to 2500 pA. Data from each cell were normalized to the response obtained with 10 μM serotonin. (■, Solid line) 2−10 measurements were made at each concentration of serotonin for a total of 86 data points from the 27 cells. Only data points where the falling phase of the current could be fit to a single-exponential process are shown. In these cells, the average rate of desensitization at saturating concentrations of serotonin was ∼0.47 s^{-1}. (△) Total (corrected) current data obtained in the same manner but from cells where a double-exponential desensitization process was observed. The fraction of the slowly desensitizing phase was 50−80% of the total current. (○) Total currents from a completely independent series of experiments with cells that showed a double-exponential desensitization process, using a total of 49 individual data points from 14 cells (2−16 measurements at each concentration were made). In this case, all traces were fit to a double-exponential desensitization process; α ranged from 3.3 to 9.1 s^{-1} (mean 5.9 ± 1.8 s^{-1}) and β from 0.27 to 0.81 s^{-1} (mean 0.48 ± 0.16 s^{-1}). The ratio of the mean rate coefficients for desensitization, α/β, is 12.4 in these experiments. Only those experiments in which the current decay could be fit to a single exponential (■) were used to calculate the parameters of the solid curve in the concentration range from 1 to 200 μM serotonin using eq 2 (Appendix). The values of the constants obtained from the best fit of these data are $\Phi = 0.09 \pm 0.03$ and $K_1 = 7.1 \pm 2.5$ μM, with a value of the maximum current amplitude, I_{max}, of 1490 pA. (•) For comparison, the dependence of the corrected whole-cell current, I_A, on the concentration of serotonin in the presence of 70 μM nicotine (dashed line) is also shown; 1−5 measurements for each data point (total 28 from 11 cells) were used to construct the dashed line. On the assumption that nicotine is a competitive inhibitor, the constants for this line were calculated using eq 4 (Appendix) and values of $\Phi = 0.09$, $K_1 = 7.1$ μM, and $I_{max} = 1750$ pA, obtained in the experiments with serotonin alone. I_{max} was calculated using the normalization point of 1300 pA obtained in the presence of 10 μM serotonin, and using eq 2. The errors in the constants were not considered in the calculations. The inhibition constant, K_X, for nicotine obtained from the best fit of the data is 19 ± 5 μM. (C) Evaluation of the cell-flow experiment with serotonin in (B) using the linear form of eq 2. (■, Solid line) The data shown as solid squares in (A) are replotted in linear form according to eq 3 (Appendix). An average value for $I_{max} = 1560$ pA from measurements in the presence of serotonin alone (see panel A), as well as in the presence of 70 μM nicotine (see panel B), was used. A linear fit of the data, including the data point after the break in the *x*-axis at 0.5 μM^{-1}, gave a slope of 2.37 ± 0.24 μM and an intercept of 0.37 ± 0.05, giving values for Φ of 0.14 ± 0.04 and for K_1 of 6.4 ± 1.8 μM for serotonin. The break in the *x*-axis is between 0.35 and 0.48 μM^{-1}.

current due to channel opening are $K_1 = 7.1 \pm 2.5$ μM, $\Phi = 0.09 \pm 0.03$, $I_{max} = 1490$ pA (reaction Scheme 1, Appendix). K_1 is the dissociation constant of the receptor site controlling channel-opening, Φ^{-1} is the channel-opening equilibrium constant, and I_{max} is the maximum current that can be obtained from one cell when all the receptor channels are open. Whether the dissociation of serotonin from AL and AL_2 (reaction Scheme 1) is the same cannot be ascertained from the experiments. The small solid circles and the dashed line in Figure 1B represent data obtained in the presence of a constant concentration (70 μM) of nicotine and will be discussed later.

For comparison with experiments with nicotine (Figure 2A) and cocaine (Figure 2B), the data represented by solid symbols and the solid line in Figure 1B are replotted in linear form in Figure 1C using eq 3 (Appendix). A Φ value of 0.14 ± 0.04 (calculated from the intercept) and a K_1 value of 6.4 ± 1.8 μM (calculated from the slope) were obtained for serotonin.

Inhibition of the 5-HT$_3$ Receptor by Nicotine. Nicotine (between 5 μM and 10 mM) alone did not activate the 5-HT$_3$ receptor on cells that contain serotonin 5-HT$_3$ receptors as demonstrated by their response to 10 μM serotonin (not shown). It did, however, inhibit serotonin-mediated whole-cell currents when co-applied with the neurotransmitter. Preincubation with nicotine for up to 20 s (data not shown) did not increase the inhibition compared to the simultaneous application with serotonin. The dashed line in Figure 1B shows the dependence of serotonin-mediated whole-cell currents in NIE-115 cells on serotonin concentration in the presence of 70 μM nicotine. The measurements defining the dashed line are indicated by the filled circles. The dose−response curve is shifted to the right, but, within experimental error, the maximum current in the presence and absence of nicotine is the same. Such a result would be expected if nicotine was a competitive inhibitor of the 5-HT$_3$ receptor, but also if it were a noncompetitive inhibitor which binds preferentially to the closed-channel forms of the receptor (see reaction Scheme 2 and eq 7b in the Appendix). There are more quantitative approaches available for differentiating between competitive and noncompetitive inhibitors (Figure 2) than the shift in the dose−response curve. These are illustrated in Figures 2 and 3.

Measurements made at a constant concentration of serotonin (10 and 200 μM in Figure 2A) and various concentrations of nicotine are illustrated in Figure 2A. Although the apparent K_I values are different at the two concentrations of serotonin, with the assumption of competitive inhibition, a

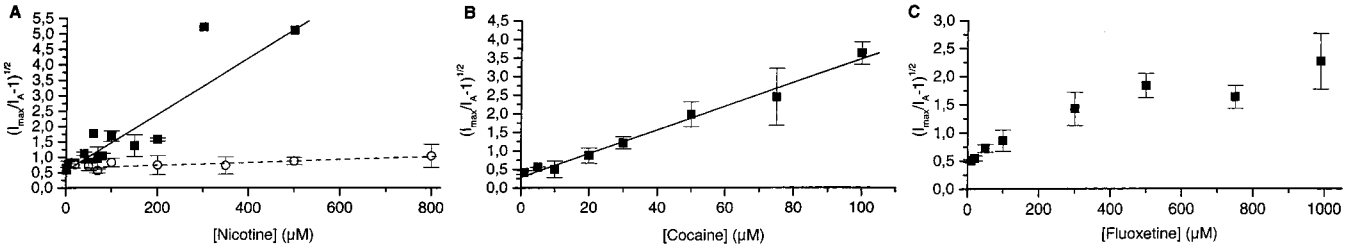

FIGURE 2: Inhibition of the 5-HT_3 receptor by nicotine and cocaine. (A) Inhibition of the 5-HT_3 receptor by nicotine at constant concentrations of serotonin. (■, Solid line) Experiments at a constant concentration of 10 μM serotonin. 1−5 measurements at each nicotine concentration (total 28 from 11 cells) were used to construct the solid line. Experimental conditions were as described in the legend to Figure 1A,B. Preincubation with nicotine (between 1 and 20 s) gave the same results as when serotonin and nicotine were equilibrated with the cell surface receptors within ca. 80 ms (data not shown). Data were plotted according to eq 5b (Appendix) using $I_{max} = 1750$ pA (see Figure 1B). The solid line is the best fit to the data (it includes the two data points obtained at high nicotine concentrations) and has a slope of 0.0092 ± 0.0009 μM and an intercept of 0.55 ± 0.12. Using a value for K_1 for serotonin of 6.4 μM (from a linear fit of the cell-flow data for serotonin in Figure 1C), a value for Φ of 0.11 ± 0.05 is obtained from the intercept of the fitted line. Using the values for K_1 and Φ from the measurements with serotonin alone (6.4 μM and 0.14, respectively, without considering the experimental error) and eq 5b, the inhibition constant, K_X, for nicotine is found to be 26 ± 3 μM. (○, Dashed line) Inhibition of the 5-HT_3 receptor by nicotine at a constant concentration of 200 μM serotonin. All other experimental conditions were as described. 1−6 measurements at each concentration of nicotine (total of 29 from 8 cells) per data point were evaluated using a value for I_{max} of 1750 pA (from Figure 1B). Data were plotted according to eq 5b; the best-fit line has a slope of 0.00048 ± 0.00017 μM^{-1} and an intercept of 0.63 ± 0.06. With $K_1 = 6.4$ μM for serotonin (from Figure 1C), a value of $\Phi = 0.37 \pm 0.07$ for serotonin was found from the intercept. Using the values for K_1 and Φ from the measurements with serotonin alone (6.4 μM and 0.14, respectively, but not considering the experimental error in the constants) and eq 5b, the inhibition constant for nicotine was found to be $K_X = 25 \pm 9$ μM. The slope of the solid line at 10 μM serotonin is 19 times larger than the slope observed at 200 μM serotonin (eq 5b). (B) Inhibition of the 5-HT_3 receptor by cocaine at a constant concentration of 10 μM serotonin. All experimental conditions were as described in (A); 2−5 measurements per data point (total of 28 from 12 different cells) were made and analyzed using eq 5b. I_{max} was determined by varying the concentration of serotonin in the constant presence of 50 μM cocaine (not shown) to be 1480 pA. The best fit of the data (solid line) had a slope of 0.032 ± 0.002 μM^{-1} and an intercept of 0.28 ± 0.1. With $K_1 = 6.4$ for serotonin, a value for Φ of 0.03 ± 0.02 was calculated from the intercept. Using the values for K_1 and Φ from the measurements with serotonin alone (6.4 μM and 0.14, respectively, but not considering the experimental error in the constants) and eq 5b, the inhibition constant, K_X, for cocaine is found to be 7.5 ± 0.5 μM. (C) Inhibition of the 5-HT_3 receptor by fluoxetine at a constant concentration of 10 μM serotonin. All experimental conditions were as described in (A). The concentration of fluoxetine was varied between 10 and 1000 μM. 2−7 measurements at each fluoxetine concentration (total of 30 measurements from 11 cells) were used in the analysis. For calculations, the average value for I_{max} of 1560 pA was used. For a noncompetitive inhibitor, a plot of $(I_{max}/I_A - 1)^{1/2}$ versus inhibitor concentration is not expected to be linear but to have a square-root dependence on inhibitor concentration, according to eq 6 (Appendix).

Table 2: Summary of Inhibition Constants for Nicotine, Cocaine, and Fluoxetine of the 5-HT_3 Receptor[a]

inhibitor	method of evaluation	figure	K_i (μM) competitive	K_i (μM) noncompetitive
nicotine	dose−response curve (eq 3)	1B	19 ± 5	
	$(I_{max}/I_A - 1)^{1/2}$ vs [nicotine] (eq 5b) at 10 μM serotonin	2A	26 ± 3	
	$(I_{max}/I_A - 1)^{1/2}$ vs [nicotine] (eq 5b) at 200 μM serotonin	2B	25 ± 9	
	$I_A/I_{A(nicotine)}$ vs [nicotine] (eq 8)	3A	28 ± 9	132 ± 38
cocaine	$(I_{max}/I_A - 1)^{1/2}$ vs [nicotine] (eq 5b) at 10 μM serotonin	2C	7.5 ± 0.5	
	$(I_{max}/I_A - 1)^{1/2}$ vs [nicotine] at 10 μM serotonin in presence of 150 μM nicotine (eq 5c)	4	8.0 ± 0.9	
	$I_A/I_{A(cocaine)}$ vs [cocaine] (eq 8)	3A	5.6 ± 1.0	26 ± 4
fluoxetine	$I_A/I_{A(fluoxetine)}$ vs [fluoxetine] (eq 7a)	3B		244 ± 24

[a] All experiments were carried out at pH 7.2, a temperature of 21−23 °C, and a transmembrane voltage of −60 mV.

serotonin concentration-independent value of K_I can be calculated. This was done by plotting and analyzing the data according to eq 5b, which was derived on the basis that nicotine is a competitive inhibitor. The observed values of Φ were 0.11 ± 0.05 and 0.37 ± 0.07 at 10 and 200 μM serotonin, respectively (Table 2). Using the K_1 and Φ values obtained for serotonin alone, the $K_I(K_X)$ value for nicotine at a serotonin concentration of 10 μM, calculated from the slope of the line, was 26 ± 3 μM, and at 200 μM serotonin concentration, it was 25 ± 9 μM (Figure 2A; Table 2). In contrast, a plot for a noncompetitive inhibitor according to eq 5b is expected to be nonlinear (eq 6). Evidence that fluoxetine is a noncompetitive inhibitor is given by the experiments in Figures 3 and 4.

Inhibition of the 5- HT_3 Receptor by Cocaine. The inhibition of the receptor by cocaine, which acts as a competitive inhibitor, is shown in Figure 2B. Preincubation with 30 μM cocaine for 100 ms or up to 30 s produced no significant increase in inhibition compared to simultaneous application of cocaine and serotonin (data not shown). Previously published experiments (*8*) indicated that the dose−response curve for serotonin and the 5-HT_3 receptor expressed in *Xenopus* oocytes is shifted to the right in the presence of 3 μM cocaine. As the serotonin concentration was increased, the affinity of the 5-HT_3 receptor for cocaine was found to decrease (*8*). However, as mentioned above, a noncompetitive inhibitor that binds preferentially to the closed-channel form can also account for these observations. One can differentiate between a competitive inhibitor and a noncompetitive inhibitor that binds mainly to the closed-channel form. Equation 6 (Appendix) shows that a plot of $(I_{max}/I_A - 1)^{1/2}$ versus the concentration of a competitive inhibitor will be linear (Figure 2A,B) but for a noncompetitive inhibitor it will be nonlinear (Figure 2C). In the case of noncompetitive inhibition, $(I_{max}/I_A - 1)^{1/2}$ is proportional to the square root of inhibitor concentration times a constant (eq 6, Appendix). This is illustrated with fluoxetine, which

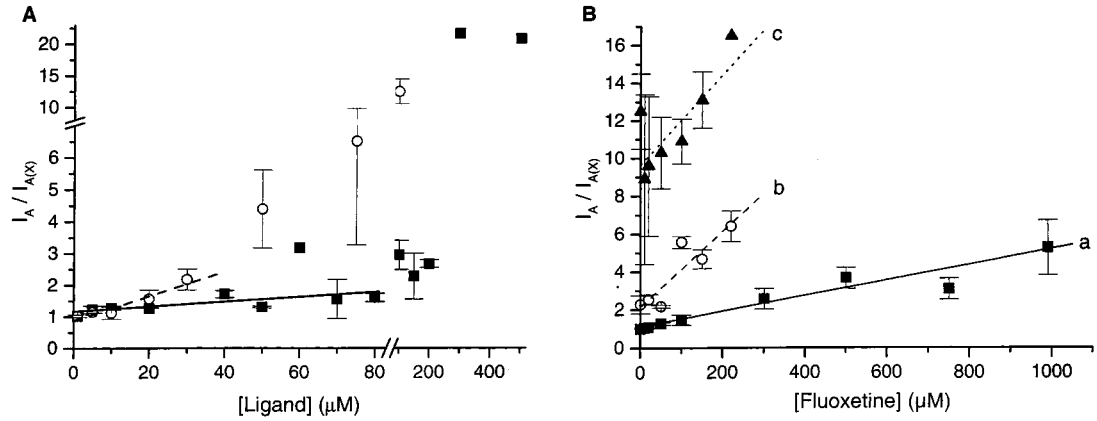

FIGURE 3: Cell-flow measurements of maximum current amplitudes corrected for receptor desensitization (*11, 13*) made with NIE-115 cells in the presence of 10 μM serotonin and the inhibitors fluoxetine, nicotine, and cocaine at pH 7.2, 21−23 °C, $V_m = -60$ mV. (A) Inhibition of the 5-HT$_3$ receptor by nicotine. (■, Solid line) 1−5 measurements (total 28 from 11 cells) were used to construct the inhibition curve (same data as in Figure 2A). A linear regression of the data up to a nicotine concentration of 80 μM gave a slope of 0.0077 ± 0.0022 μM^{-1} and an intercept of 1.18 ± 0.16. The apparent inhibition constant, K_X (from eq 7a), is 132 ± 38 μM. The data were analyzed by treating nicotine as a competitive inhibitor, using eq 8 and neglecting the contribution of $F_A(X/K_X)$. From this analysis, using the data up to 80 μM nicotine only, an inhibition constant, K_X, of 28 ± 9 μM was obtained for nicotine. (○, Dashed line) Inhibition by cocaine. The dashed line was constructed using 2−5 measurements per data point (total 28) from 12 cells (same data as in Figure 2B). Only data points up to a concentration of 30 μM cocaine were used for analysis. The slope of the fitted line is 0.038 ± 0.006 μM^{-1}, and the intercept is 0.88 ± 0.11. Using eq 7a, an apparent inhibition constant K_X of 26 ± 4 μM was found. Applying eq 8 and treating cocaine as competitive inhibitor gave an inhibition constant K_X of 5.6 ± 1.0 μM. The break in the *x*-axis is between 83 and 95 μM inhibitor concentration and the break in the *y*-axis [$I_A/I_{A(X)}$] between 7 and 8. Note the deviation from linearity at higher concentrations of inhibitor in both cases. (B) Inhibition of the 5-HT$_3$ receptor by fluoxetine alone and in the presence of nicotine and cocaine at a constant concentration of 10 μM serotonin, pH 7.2, 21−23 °C, $V_m = -60$ mV. Curve a (■, solid line): The solid squares and solid line represent data from 2−7 measurements at each fluoxetine concentration (total of 30 measurements from 11 cells). The solid line has a slope of 0.0041 ± 0.0004 μM^{-1} and an intercept of 1.11 ± 0.17; using eq 7a, an apparent inhibition constant K_X of 244 ± 24 μM was obtained. Note that the linear relation is still valid at higher inhibitor concentrations (up to 4 × $K_{X,app.}$). Curve b (○, dashed line): Inhibition of the receptor by fluoxetine in the presence of 70 μM nicotine; 2−3 measurements at each concentration, for a total of 16 measurements from 5 cells, were used to construct the dashed line. A linear regression of the data gave a slope of 0.020 ± 0.005 μM^{-1} and an intercept of 2.14 ± 0.57. Curve c (▲, dotted line): Inhibition of the receptor by fluoxetine in the presence of 100 μM cocaine using 3−4 measurements at each concentration for a total of 23 data points from 7 cells. A linear regression of the data gave a slope of 0.024 ± 0.011 μM^{-1} and an intercept of 9.64 ± 0.97.

behaves as a typical noncompetitive inhibitor. As can be seen in Figure 2C, a plot of $(I_{max}/I_A - 1)^{1/2}$ versus fluoxetine concentration is not linear (according to eq 6, Appendix). Further evidence that cocaine and nicotine are competitive inhibitors of the receptor and that fluoxetine does not compete with cocaine or nicotine for their binding sites on the receptor is given in Figures 3 and 4. The linear relationship between $(I_{max}/I_A - 1)^{1/2}$ and cocaine concentration is consistent with cocaine being a competitive inhibitor (Figure 2B; eq 5b, Appendix). Using the values of K_1 and Φ obtained in the presence of serotonin alone, and a value of 1480 pA for I_{max}, a $K_I(K_X)$ value of 7.5 ± 0.5 μM for cocaine was calculated using eq 5b (Appendix) (Table 2).

Measuring the ratio of the current amplitudes obtained in cell-flow experiments, corrected for receptor desensitization, in the absence, I_A, and presence $I_{A(X)}$, of inhibitor (see eq 7) can give additional information about the inhibition mechanism. A linear relationship (eq 7a, Appendix) exists between $I_A/I_{A(X)}$ and noncompetitive inhibitor concentration over a wide concentration range (see experiments with fluoxetine, Figure 3B, curve a). In the case of a competitive inhibitor, however, the plot of the ratio of $I_A/I_{A(X)}$ versus competitive inhibitor concentration is expected to be linear only at low inhibitor concentrations, when $F_A(X/K_X)$ in eq 8 is small compared to $2F_A + F_{AL}$. F_A and F_{AL} represent the fraction of receptors in form A or AL (reaction Scheme 1, Appendix), respectively. Figure 3A shows plots of $I_A/I_{A(X)}$ versus nicotine (solid symbols) or cocaine (open symbols) concentration at a constant concentration (10 μM) of serotonin according to eq 8. As is expected for competitive inhibitors, a linear relationship between $I_A/I_{A(X)}$ and nicotine or cocaine concentration was obtained only at low inhibitor concentration: in the range of nicotine concentration from 0 to 80 μM (solid line in Figure 3A) and of cocaine concentration from 0 to 30 μM (dashed line in Figure 3A). The values for F_A and F_{AL} were calculated using the K_1 and Φ values obtained for serotonin alone (Figure 1C). The inhibition constants obtained at low concentrations of the inhibitor for nicotine (solid line in Figure 3A) and cocaine (dashed line in Figure 3A) and calculated by using eq 8 were found to be 28 ± 9 and 5.6 ± 1.0 μM, respectively. These values are in agreement with those obtained from the measurements shown in Figure 2A,B (Table 2).

Inhibition of the 5-HT$_3$ Receptor by Fluoxetine. In contrast to the $I_A/I_{A(X)}$ versus inhibitor concentration plots with the inhibitors nicotine and cocaine, which are linear only at low inhibitor concentrations, are plots with fluoxetine as the inhibitor (curve a, Figure 3B). Inhibition of the 5-HT$_3$ receptor in neurons of rat nodose ganglia by fluoxetine has been observed previously (*9*). Whether this inhibition is competitive or noncompetitive with serotonin was not determined. The results shown in Figure 3B indicate that fluoxetine is a noncompetitive inhibitor of the 5-HT$_3$ receptor in NIE-115 cells in the concentration range from 1 to 1000 μM fluoxetine (curve a, Figure 3B). An apparent inhibition constant of $K_Y = 244 \pm 24$ μM was determined. As is expected for a noncompetitive inhibitor (eq 7a, Appendix), the relationship between $I_A/I_{A(X)}$ and inhibitor concentration is linear over a 1000-fold concentration range of fluoxetine. In agreement with previous observations with neurons from

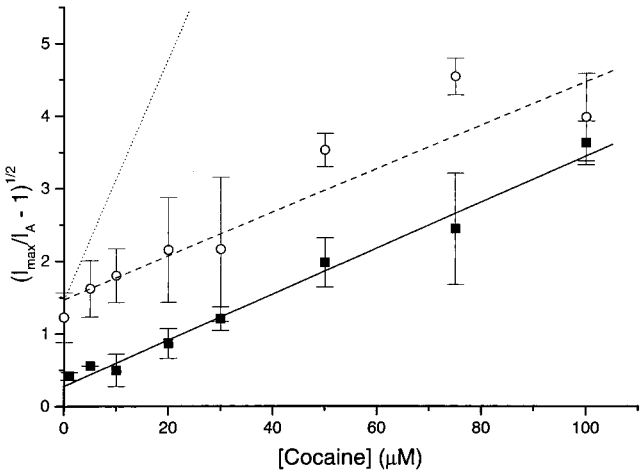

FIGURE 4: Inhibition of the 5-HT_3 receptor by cocaine in the presence of nicotine at a constant concentration (10 μM) of serotonin, pH 7.2, 21−23 °C, $V_m = -60$ mV. (■, Solid line) Inhibition of the 5-HT_3 receptor by cocaine alone. For comparison, the data and regression line from Figure 2C are replotted (see legend to Figure 2C for details). (○, Dashed line) Inhibition of the receptor by cocaine in the presence of 150 μM nicotine; 2−5 measurements at each cocaine concentration (total of 30 from 7 cells) were used in the analysis. The best fit to the data (dashed line) has a slope of $0.030 \pm 0.003\ \mu M^{-1}$ and an intercept of 1.47 ± 0.15. Using values for K_1 and Φ for serotonin of 6.4 and 0.14, respectively (as determined in Figure 1C, and not considering the error in the constants in the calculation), the case of two competitive inhibitors applied simultaneously can be analyzed using eq 5c (Appendix). From the intercept, an inhibition constant, K_X, for nicotine of $42 \pm 4\ \mu$M was found. From the slope, an inhibition constant, K_X, for cocaine of $8.0 \pm 0.9\ \mu$M was calculated. The dotted line is a simulation for the case in which nicotine and cocaine both compete with serotonin for the agonist-binding site but do not compete with each other for binding to the receptor. In this case, eq 5d (Appendix) applies. The dotted line was calculated using eq 5d, the K_X values for nicotine (42 μM) determined in this experiment, and an average K_X value for cocaine (6.6 μM) calculated from the experiments listed in Table 2.

rat nodose ganglia (*9*), we observed that inhibition by fluoxetine of the 5-HT_3 receptor in NIE-115 cells is time-dependent. A fast inhibition process occurs within the mixing time of the cell-flow device of 80−100 ms. After preincubation of the NIE-115 cells with 100 μM fluoxetine for up to 20 s, additional inhibition of the 5-HT_3 receptor is observed. This inhibition process with a time constant for formation of the receptor−inhibitor complex of approximately 15 s is not considered here. Investigations of the inhibition of the nicotinic acetylcholine receptor in BC_3H1 cells by the anticonvulsant MK-801 also revealed a rapid and a slow inhibition reaction (*24*).

Simultaneous Application of Two Inhibitors. The hypothesis that fluoxetine is a noncompetitive inhibitor and binds to a different binding site on the serotonin receptor than the site to which nicotine and cocaine bind was examined further in the measurements shown in Figure 3B. In mixed inhibition experiments, constant concentrations of serotonin and a constant concentration of one inhibitor, X, and varying amounts of a second inhibitor, Y, were simultaneously equilibrated with the receptors. These experiments were performed to determine if nicotine and fluoxetine, or cocaine and fluoxetine, bind to the same or independent sites on the receptor. The measurements obtained at constant serotonin (10 μM) and constant nicotine ($X = 70\ \mu$M) concentration as a function of fluoxetine concentration are shown in Figure 3B (curve b; ○, dashed line). If nicotine and fluoxetine are both noncompetitive inhibitors, and bind to the same site, the slope of the $I_A/I_{A(X)}$ plot is expected to be the same in the absence and presence of nicotine (eq 9). This is not observed; curve a (fluoxetine alone) has a slope of $0.004 \pm 0.0005\ \mu M^{-1}$, giving a value for the apparent K_X of $244 \pm 24\ \mu$M, while for curve b (constant concentration of 70 μM nicotine) the slope has increased by a factor of ~4 to $0.020 \pm 0.005\ \mu M^{-1}$. This indicates that nicotine does not bind to the same site as the noncompetitive inhibitor fluoxetine (compare eqs 9 and 10). Curve c in Figure 3B represents data obtained at constant concentrations of serotonin (10 μM) and cocaine ($X = 100\ \mu$M). Similar results to those obtained with nicotine (curve b) were obtained with cocaine. In the presence of 100 μM cocaine (curve c), the slope of the line increased by a factor of ~5 to $0.025 \pm 0.011\ \mu M^{-1}$ compared to the slope of the line obtained with fluoxetine alone (curve a). This indicates that cocaine does not bind to the same site as fluoxetine. These experiments are consistent with the experiments described earlier showing that nicotine and cocaine are competitive inhibitors, which are not expected to bind to the same site as the noncompetitive inhibitor fluoxetine.

The evidence shown so far indicates that nicotine and cocaine are competitive inhibitors of the 5-HT_3 receptor on NIE-115 cells. To further confirm this hypothesis, measurements were carried out to determine whether nicotine and cocaine bind to the same site. In these experiments, a constant concentration of nicotine (150 μM) and varying concentrations of cocaine were used. The serotonin concentration was held constant at 10 μM (Figure 4, solid line). If the two competitive inhibitors bind to the same site on the receptor, eq 5c (Appendix) applies. In this case, one would expect the intercept of the $(I_{max}/I_A - 1)^{1/2}$ versus cocaine concentration plot to change, but the slope to remain the same, in the presence and absence of 150 μM nicotine. This is observed (Figure 4, broken line). Using the values of K_1 and Φ obtained in the presence of serotonin alone, a value of 1480 pA for I_{max}, and eq 5c (Appendix), the value of the inhibition constant, K_X, for cocaine calculated from the slope of the line was found to be $8.0 \pm 0.9\ \mu$M. In the absence of 150 μM nicotine, the K_X value for cocaine was found to be $7.5 \pm 0.5\ \mu$M (Figure 2B). These values agree, within experimental error, with those found when only one or the other inhibitor is present (Table 2) and are consistent with a mechanism in which nicotine and cocaine bind to the same site on the receptor. An alternative mechanism in which both nicotine and cocaine compete with serotonin but occupy independent sites is not consistent with the results in Figure 4. As nicotine and cocaine are competitive inhibitors by themselves, it is assumed that the presence of only one inhibitor prevents serotonin from binding. If nicotine and cocaine bind to separate sites one would expect a change of both the slope and the intercept in the $(I_{max}/I_A - 1)^{1/2}$ versus cocaine concentration plot (eq 5d, Appendix). The slope would be multiplied by the factor $(1 + X/K_X)$, where the inhibitor concentration X remains constant and K_X is its dissociation constant. The dotted line in Figure 4 is a simulation for this mechanism where cocaine and nicotine are both competitive inhibitors but they bind to different sites on the receptor. The line was calculated using K_1 and Φ values obtained with serotonin alone, and an inhibition

constant K_X of 42 μM for nicotine and of 6.6 μM (average of previous determinations, see Table 2) for cocaine.

The results in Figures 2A,B and 3A,B are all consistent with nicotine and cocaine being competitive inhibitors of the 5-HT$_3$ receptor. The experiments also indicate that these competitive inhibitors do not bind to the same site as fluoxetine does (Figure 3B). This is consistent with the experiments shown in Figures 2C and 3B (curve a) that indicate that fluoxetine is a noncompetitive inhibitor. The experiments illustrated in Figure 4 further support these conclusions by indicating that nicotine and cocaine bind to the same site on the 5-HT$_3$ receptor. The observed competitive and noncompetitive inhibitor dissociation constants, K_I, obtained under different experimental conditions agree and are summarized in Table 2. The possibility that the competitive inhibitors bind to different sites on different conformations of the protein in equilibrium with each other, so that occupancy of one site prevents binding to the other site, is not excluded by the experiments.

DISCUSSION

The mechanism of the 5-HT$_3$ receptor on NIE-115 cells was investigated using a rapid reaction technique with a 10 ms time resolution. In this study, only the inhibition of the slowly desensitizing receptor form, with an average desensitization rate constant in the presence of 10 μM serotonin of 0.47 s^{-1}, was investigated. The technique involves flowing ligand solutions over the cell (*10*), using the whole-cell current-recording technique (*12*) to determine the current due to opening of receptor-channels, and correcting the observed current for desensitization that occurs while the receptors on the cell surface equilibrate with serotonin (*11, 13*).

The results indicate that the same minimum mechanism (reaction Scheme 1, Appendix) that accounts for channel opening of the nicotinic acetylcholine (*11, 15, 25*), GABA$_A$ (*19*), and glycine (*20*) receptors also accounts for the results obtained with the serotonin 5-HT$_3$ receptor in NIE-115 cells. That desensitization of the 5-HT$_3$ receptor is a complex process and occurs in two time regions has been reported previously (*6, 7*). The results presented here (Table 1) indicate that the two desensitization processes are due to two independent forms of the 5-HT$_3$ receptor, which do not interconvert on the time scale (10 s) of our experiments. Similar results have been obtained in experiments with the GABA$_A$ (*19, 23*) and glycine (*20*) receptors.

In light of the conclusion that two receptor forms that do not interconvert exist in NIE-115 cells, it should be noticed that the dependence of the maximum current amplitude on serotonin concentration (Figure 1B) in cells which contain only one receptor form (solid symbols) is similar to that obtained with cells which contain two receptor forms (open symbols). This observation can be accounted for by similar receptor−serotonin dissociation constants K_1 (reaction Scheme 1) of the two forms. It is of interest, therefore, to note that phosphorylation of the nicotinic acetylcholine receptor from *Torpedo californica* by a cAMP-dependent protein kinase results in a decreased desensitization rate without a change in the receptor−acetylcholine dissociation constant (*26*). Several reagents with completely different modes of action on the cyclic AMP system were found to modulate the amplitude and desensitization rate of 5-HT$_3$ receptor-mediated whole-cell currents in clonal (NG108-15) cells (*6, 27*). The sequence of a cloned 5-HT$_3$ receptor subunit suggests the presence of phosphorylation sites (*5*). Phosphorylation was shown to control the single-channel conductance of the 5-HT$_3$ receptor in NIE-115 cells (*28*). The value we measured for the single-channel (slope) conductance of 7.1 pS for the 5-HT$_3$ receptor on NIE-115 cells in the cell-attached mode (data not shown) is in agreement with values reported previously (*4, 5, 29*).

Cocaine, an abused drug (*30*), and fluoxetine, used clinically to treat depression (see, for instance, refs *3, 31*), were used here to help us understand the mechanism by which nicotine inhibits the serotonin receptor. It has been reported that cocaine is a competitive inhibitor of the 5-HT$_3$ receptor on the basis that the receptor affinity for cocaine decreased as the serotonin concentration was increased (*8*). A similar observation was made in the investigation of cocaine, a noncompetitive inhibitor of the muscle-type nicotinic acetylcholine receptor in BC$_3$H1 cells (*22*). In these experiments, cocaine has a 6-fold higher affinity for the closed-channel form than the open-channel form of the receptor. Consequently, the affinity for cocaine decreases as the concentration of channel-activating ligand increases. The same is expected if cocaine were a competitive inhibitor. The experiments in Figures 2B and 3A (open symbols) differentiate between a noncompetitive inhibitor with properties similar to cocaine on muscle nicotinic acetylcholine receptors, which binds with much higher affinity to closed-channel forms than it does to the open-channel form of the acetylcholine receptor (*22*), and a competitive inhibitor. Both experiments (Figures 2B and 3A) are consistent with cocaine being a competitive inhibitor of the 5-HT$_3$ serotonin receptor and give similar dissociation constants of 7.5 and 5.6 μM (Table 2).

The widely used antidepressant fluoxetine, an inhibitor of serotonin uptake (*3*), also inhibits the 5-HT$_3$ receptor in isolated rat nodose ganglion neurons (*9*). The mechanism of this inhibition was not determined in those experiments. We have observed two processes with fluoxetine; the one we have characterized occurs within the mixing time of the rapid mixing device (~80 ms). An additional slower inhibition process is also observed after preincubation of NIE-115 cells with 100 μM fluoxetine for 5−20 s, and is associated with a higher affinity of the receptor for the inhibitor. We have not yet examined the slow inhibition process. It should be noted that in our studies on NIE-115 cells, the inhibition constant of fluoxetine is around 244 μM, while on rat nodose ganglion neurons an IC_{50} of 1.2 μM was found for fluoxetine (*9*). This might be due to the different tissues used in the experiments which may contain different isoforms of the receptor. Differences in the ligand-binding properties of the 5-HT$_3$ receptor in different tissues have been reported (*32, 33*). Fluoxetine binds to 5-HT$_3$ receptors on rat cortical membranes with high affinity (*32*); IC_{50} values for displacement of the radioligands [^{3}H]-quipazine and [^{3}H]paroxetine were 10 ± 2 and 15 ± 2 nM, respectively (*32*). However, when displacement of [^{3}H]-zacopride on rat entorhinal cortices, or of [^{3}H]ICS 205-930 on NIE-115 cells, was studied, the affinity for fluoxetine was lower by a factor of ca. 1000 (*33*). In the equilibrium experiments, in which displacement of a radioligand is used to determine the affinity of an inhibitor like fluoxetine, it is

not known whether the measurements reflect the binding to the receptor before or after desensitization, or even binding to sites other than on the serotonin receptor. These ambiguities are avoided in kinetic experiments where one measures the effect of the specific receptor ligand serotonin and an inhibitor on the current resulting from the opening of serotonin-activated transmembrane channels.

From Figures 2C and 3B (curve a), it can be seen that fluoxetine has the characteristics of a noncompetitive inhibitor. In contrast to the measurements with nicotine and cocaine, $I_A/I_{A(X)}$ versus inhibitor concentration plots are linear over a 1000-fold range of fluoxetine concentration (Figure 3B, curve a), and a plot of $(I_{max}/I_A - 1)^{1/2}$ versus inhibitor concentration is not linear, as is expected for a noncompetitive inhibitor (eq 6, Appendix) (Figure 2C). Additionally, the experiments indicate (Figure 3B) that neither nicotine (curve b) nor cocaine (curve c), which act like competitive inhibitors, occupy the same or an interacting binding site as the noncompetitive inhibitor fluoxetine (Figure 3B, curves b and c; eqs 9 and 10, Appendix).

The inhibition of the 5-HT_3 receptor by nicotine has not been reported previously. The preponderance of the evidence obtained from the experiments discussed demonstrates that nicotine is a competitive inhibitor of the 5-HT_3 receptor on NIE-115 cells: (i) the plots of $(I_{max}/I_A - 1)^{1/2}$ versus nicotine concentration in the presence of constant concentrations of serotonin are linear (Figure 2A); (ii) nicotine inhibition can be overcome by high serotonin concentrations (Figure 1B); (iii) nicotine and fluoxetine, a noncompetitive inhibitor, do not occupy the same or interacting binding sites on the receptor (Figure 3B, curve b); (iv) nicotine and cocaine occupy the same binding site (Figure 4); and (v) on the assumption of competitive binding, different treatment of the data (Figures 2A and 3A, solid line) gives essentially the same observed value for the inhibition constant for nicotine (Table 2).

How do the observed inhibition constants relate to clinical situations? Blood plasma levels of nicotine in smokers are normally around 10 ng/mL, corresponding to a plasma concentration of ca. 0.06 μM nicotine (*34*). Shortly after smoking, plasma levels of nicotine are around 0.15 μM (25 ng/mL), and may reach 1 μM during inhalation (*34*). Plasma levels of cocaine vary strongly, depending on the mthod of drug administration. Oral or intranasal administration (chewing or snorting) produces blood plasma levels of ca. 0.5 μM cocaine (150 ng/mL, *35*); smoking or intrapulmonary application can create plasma concentrations of 1−3 μM (300−900 ng/mL) cocaine (*35*). Intravenous administration usually produces a plasma concentration of ca. 1 μM cocaine; in heavy users plasma levels of cocaine may reach up to 5 μM (1500 ng/mL) cocaine (*35*). In the case of fluoxetine, plasma levels of ca. 1 μM are commonly attained through medication (*9*). According to these figures, major effects on the function of the 5-HT_3 receptor would only be expected from cocaine (observed K_X ca. 7.5 μM, plasma levels in users 1−5 μM), while in the case of nicotine and fluoxetine the K_X values found are higher than their effective doses by a factor of 20−100 (observed K_X ca. 25 μM, plasma levels in users 0.1−1 μM for nicotine; observed K_X ca. 244 μM, plasma levels in patients ca. 1 μM for fluoxetine). It must be noted, however, that in the case of fluoxetine dramatic variations in receptor affinity, differing by a factor of 1000, were reported (see above); similar effects may apply in the case of nicotine and cocaine. While the available information does not let one decide whether the specific inhibitors chosen for these studies have important physiological roles in modifying the 5-HT_3 receptor, characterization of the receptor inhibition sites is important for an understanding of the receptor's role in signal transmission.

The effect of nicotine on the 5-HT_3 serotonin receptor is of interest for several reasons. (i) Results from molecular biology studies indicate that members of the ligand-gated neurotransmitter receptor superfamily, including the nicotinic acetylcholine receptor, come from common ancestral genes (*36*−*38*). Observed effects of serotonergic agents on neuronal nicotinic acetylcholine receptors (*39*), as well as the study of chimaeric nicotinic acetylcholine−5-HT_3 receptor channels expressed in *Xenopus* oocytes (*40*), indicate close similarity of topology and function of these two receptors despite different agonist-binding sites and ion permeabilities. Here we show that nicotine, an activating ligand of the nicotinic acetylcholine receptor (*41*), binds to apparently the same site as serotonin does on the 5-HT_3 receptor in NIE-115 cells. But the binding of nicotine to the serotonin site does not lead to channel opening. (ii) Nicotine and cocaine are both competitive inhibitors of the serotonin receptor, even though cocaine is a noncompetitive inhibitor of the nicotinic acetylcholine receptor in BC_3H1 cells (*22*). It is also of interest to note that in addition to nicotine being an activator of the acetylcholine receptor in BC_3H1 cells, it also binds to an inhibitory site (Bremer and Hess, unpublished results). Whether this inhibitory site of the acetylcholine receptor coincides with the cocaine site is not yet known. (iii) Since most addictive drugs affect brain dopamine levels (reviewed in *42*), and brain 5-HT_3 receptors are known to be involved in this regulatory circuitry, the effect of nicotine on the 5-HT_3 receptor is also expected to affect brain dopamine levels. Dopamine itself has been reported to elicit a 5-HT_3 receptor-mediated response in NIE-115 cells (*43*). Our results demonstrate a direct biochemical involvement of nicotine in serotonergic/dopaminergic circuits in the brain which may be of relevance in the consideration of drug addiction.

In contrast to nicotine and cocaine, fluoxetine is a noncompetitive inhibitor of the serotonin receptor (Figure 3, curve a) and acts on a different site than nicotine and cocaine do (Figure 3, curves b and c). In this regard, it is of interest that fluoxetine also inhibits the serotonin transporter (*44*), which is important in regulating brain serotonin responses (*45*) and, therefore, the brain dopamine levels, which are affected by addictive drugs (reviewed in *42*).

Evidence gathered so far (see also *42*) shows that nicotine has major effects on brain centers and pathways that are also regulated by 5-HT_3 receptors. This study demonstrates a direct action of nicotine on the 5-HT_3 receptor; this has not been reported previously. The fact that with respect to the 5-HT_3 receptor nicotine acts in a similar way to cocaine also indicates that the pharmacological effects of nicotine are similar to those of other addictive drugs, and that nicotine targets sites in those centers of the brain that are also targeted by a large number of both therapeutic and abused compounds (*46*). The cell flow technique with a 10 ms time resolution (*11*) allows one to decide whether inhibitors bind to a single or multiple binding site(s), whether they are competitive or

Scheme 1

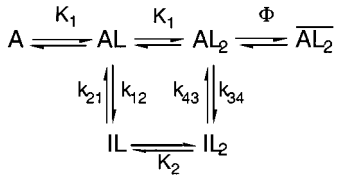

noncompetitive, and whether two different inhibitors bind to the same or independent sites. The recently developed laser-pulse photolysis technique (*18, 47*−*49*), which has a 100-fold better time resolution than the cell-flow technique, gives additional, essential information about the rate constants for channel-opening (k_{op}) and channel-closing (k_{cl}). It also gives information about the effect of inhibitors on k_{op} and k_{cl}, and, therefore, on the channel-opening equilibrium constant ($\Phi = k_{op}/k_{cl}$). In the laser-pulse photolysis technique, biologically inert photolabile precursors of the neurotransmitter (caged neurotransmitters) are equilibrated with receptors on the cell surface and photolyzed to liberate the neurotransmitter in the microsecond time region. Such compounds have been used and are available for investigations of the excitatory acetylcholine, glutamate, and kainate receptors and the inhibitory γ-aminobutyric (GABA) and glycine receptors (reviewed in *48* and *49*). The synthesis, photochemistry, and biological properties of a biologically inert photolabile serotonin derivative suitable for investigating the 5-HT$_3$ serotonin receptor have been described (*50*).

The recently developed rapid chemical reaction techniques for investigating neurotransmitter-mediated reactions on cell surfaces in the microsecond to millisecond time region may, therefore, be useful in answering many of the remaining questions regarding the chemical mechanism of neurotransmitter-mediated reactions and the chemical mechanisms by which these receptors are inhibited by a large number of clinically relevant and abused compounds (*46*).

ACKNOWLEDGMENT

We thank Jue Lin for help with preliminary nicotine experiments, Dr. Marshall Nirenberg (NIH, Bethesda, MD) for a gift of NIE-115 mouse neuroblastoma cells, and Dr. H. P. M. Vijverberg (University of Utrecht, Netherlands) for helpful suggestions regarding cell culture and maintenance.

APPENDIX: MECHANISMS AND EQUATIONS USED FOR DATA ANALYSIS

Reaction Scheme 1. In the minimum reaction scheme for the serotonin 5-HT$_3$ receptor in NIE-115 mouse neuroblastoma cells, the binding of two neurotransmitter molecules before the channel opens is required. The binding of two ligand molecules before the channel opens is also required in various forms of the excitatory acetylcholine receptor (*11, 15, 25*) and the inhibitory γ-aminobutyric acid (GABA$_A$) (*19*) and glycine (*20*) receptors in mouse cerebral cortical and spinal cord cells, respectively.

A represents the active, nondesensitized receptor and L the neurotransmitter; the subscript 2 indicates the number of ligand molecules bound. $\overline{AL_2}$ is the open-channel form of the receptor, and I denotes the desensitized, inactive receptor. K_1 is the dissociation constant of the receptor site controlling channel-opening, K_2 is the dissociation constant

Scheme 2

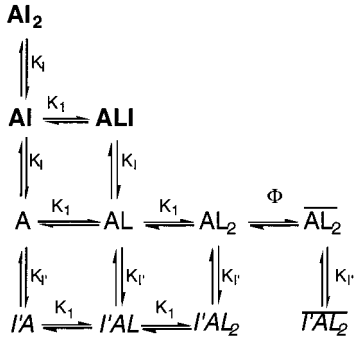

of the ligand from the desensitized receptor, and Φ^{-1} is the channel-opening equilibrium constant. Only the rate constant k_{34} is usually sufficient to describe receptor desensitization. The direct conversion of the A or $\overline{AL_2}$ form to transiently inactivated, desensitized receptor forms is neither included nor excluded by the measurements. This reaction scheme has been shown to account for the opening mechanism of the muscle type of the excitatory nicotinic acetylcholine receptor in the electric organ of *Electrophorus electricus* (*25*) and *Torpedo californica* (*51*) and in BC$_3$H1 cells (*11*), and of the inhibitory GABA$_A$ (*19*) and glycine (*20*) receptors.

The observed whole-cell current in the experiments reported here is a measure of the concentration of open receptor-channels. Correction of the whole-cell current for desensitization during equilibration with ligand is given by (*11, 13*):

$$I_A = (e^{\alpha\Delta T} - 1)\sum_{i=1}^{n}(I_{obs})_{\Delta ti} + (I_{obs})_{\Delta tn} \qquad (1)$$

I_A denotes the current amplitude corrected for receptor desensitization. $(I_{obs})_{\Delta ti}$ is the observed current during the ith time interval and $(I_{obs})_{\Delta tn}$ the observed current in a time interval equal to or greater than the time needed to reach the maximum current. When the time constant for reaching the observed maximum current amplitude in cell-flow experiments, indicative of equilibration of cell surface receptors with the ligand solution emerging from the flow device, was much smaller (approximately a factor of 10) than the time constant for the slowly desensitizing phase (when two phases were observed), the current amplitude of that phase was corrected by a linear extrapolation to zero time.

Mechanism Used for Inhibition Studies. In reaction Scheme 2 **I** represents the competitive inhibitor and I' the noncompetitive inhibitor. K_I and $K_{I'}$ are dissociation constants for **I** and I', respectively. It is assumed in the model that there exists only a single dissociation constant for the noncompetitive inhibitor (for instance, I' binds equally well to A, AL, AI$_2$, and AL$_2$ in Scheme 2).

Dose−*Response Curve (Nonlinear Fit) (11)*:

$$I_A = \frac{I_{max}}{\left[\frac{K_1}{L} + 1\right]^2 \Phi + 1} \qquad (2)$$

I_{max} is the maximum current that can be obtained from one cell when all the receptor channels are open. K_1 is the dissociation constant of the neurotransmitter from the receptor, Φ^{-1} is the channel-opening equilibrium constant, and L

denotes the concentration of activating ligand. In deriving this equation, it is assumed that the neurotransmitter concentration, L, is much larger than the concentration of ligand binding sites, and that these binding sites are characterized by a single dissociation constant, K_1 (*17*). This equation can be linearized (*17*):

$$\left(\frac{I_{max}}{I_A} - 1\right)^{1/2} = \Phi^{1/2} + \frac{K_1}{\mathbf{L}}\Phi^{1/2} \quad (3)$$

Dose−Response Curve in the Presence of a Competitive Inhibitor:

$$I_A = \frac{I_{max}}{\left[\frac{K_1}{L}\left(1 + \frac{X}{K_X}\right) + 1\right]^2 \Phi + 1} \quad (4)$$

X is the concentration of inhibitor, K_X is the inhibition constant, and all the other constants are as described before. When the inhibitor concentration **X** is constant and the ligand concentration **L** is varied, eq 4 can be linearized:

$$\left(\frac{I_{max}}{I_A} - 1\right)^{1/2} = \Phi^{1/2} + \frac{K_1}{\mathbf{L}}\Phi^{1/2}\left(1 + \frac{X}{K_X}\right) \quad (5a)$$

When the ligand concentration **L** is constant and the inhibitor concentration **X** is varied, eq 4 can be rearranged to study the dependence of the whole-cell current on inhibitor concentration:

$$\left(\frac{I_{max}}{I_A} - 1\right)^{1/2} = \Phi^{1/2}\left(1 + \frac{K_1}{L}\right) + \frac{X}{K_X}\frac{K_1}{L}\Phi^{1/2} \quad (5b)$$

In the presence of two competitive inhibitors, both binding to the same site on the receptor, and when the concentrations of ligand L and of inhibitor X are constant but that of inhibitor **Y** is varied, eq 5b becomes

$$\left(\frac{I_{max}}{I_A} - 1\right)^{1/2} = \Phi^{1/2}\left[1 + \frac{K_1}{L}\left(1 + \frac{X}{K_X}\right)\right] + \frac{\mathbf{Y}}{K_Y}\frac{K_1}{L}\Phi^{1/2} \quad (5c)$$

If two competitive inhibitors bind to different sites on the receptor (but both still compete with the activating ligand), this equation would be:

$$\left(\frac{I_{max}}{I_A} - 1\right)^{1/2} = \Phi^{1/2}\left[1 + \frac{K_1}{L}\left(1 + \frac{X}{K_X}\right)\right] + \frac{\mathbf{Y}}{K_Y}\left(1 + \frac{X}{K_X}\right)\frac{K_1}{L}\Phi^{1/2} \quad (5d)$$

providing the concentrations of ligand L and inhibitor X are constant and the concentration of inhibitor **Y** is varied.

Noncompetitive Inhibition (52, Equation 7a):

$$\left(\frac{I_{max}}{I_A} - 1\right)^{1/2} = \left(\Phi^{1/2} + \frac{K_1}{\mathbf{L}}\Phi^{1/2}\right)Z \quad (6)$$

Here $Z = \sqrt{(X/K_X)(1/1-\overline{FAL_2})}$ when the noncompetitive inhibitor X binds to all forms of the receptor and $Z = \sqrt{X/K_X+1}$ when the noncompetitive inhibitor binds only to the closed-channel forms of the receptor.

General Noncompetitive Inhibition:

$$\frac{I_A}{I_{A(X)}} = 1 + \frac{X}{K_X} \quad (7a)$$

In the case of a noncompetitive inhibitor which binds preferentially to the closed-channel form of the receptor, eq 7b applies:

$$\frac{I_A}{I_{A(X)}} = 1 + \frac{X}{K_X}(1 - F_{\overline{AL_2}}) \quad (7b)$$

X represents the concentration of the noncompetitive inhibitor, and K_X is the inhibition constant. I_A is the maximum whole-cell current corrected for receptor desensitization at a given concentration of serotonin and $I_{A(X)}$ the corrected maximum current amplitude at the same concentration of serotonin in the presence of inhibitor X. $F_{\overline{AL_2}}$ is the fraction of the receptors in the open-channel form. In eq 7b, at high serotonin concentrations when $F_{\overline{AL_2}} \rightarrow 1$, $I_A/I_{A(X)}$ approaches 1.

Competitive Inhibition:

$$\frac{I_A}{I_{A(X)}} = 1 + \frac{X}{K_X}\left[(2F_A + F_{AL}) + F_A\frac{X}{K_X}\right] \quad (8)$$

X represents the concentration of inhibitor, and K_X is the inhibition constant. F_A and F_{AL} are the fractions of unliganded and singly liganded receptor species at equilibrium, respectively:

$$F_A = \frac{\left(\frac{K_1}{L}\right)^2\Phi}{\left(\frac{K_1}{L+1}\right)^2\Phi + 1}$$

$$F_{AL} = \frac{2\left(\frac{K_1}{L}\right)\Phi}{\left(\frac{K_1}{L} + 1\right)^2\Phi + 1}$$

It should be noticed that the equation for competitive inhibitors reduces to that of noncompetitive inhibitors when the term $F_A(X/K_X) \ll (2F_A + F_{AL})$ in eq 8, that is, at low inhibitor concentration (Figure 3A).

Inhibition When Two Inhibitors Are Applied Simultaneously. When two noncompetitive inhibitors bind to the same site (*53*):

$$\frac{I_A}{I_{A(X,Y)}} = 1 + \frac{X}{K_X} + \frac{Y}{K_Y} \quad (9)$$

X and Y represent the concentrations of the noncompetitive inhibitors, and K_X and K_Y are the corresponding inhibition constants. In the case of noncompetitive inhibitors binding to different sites on the receptor, eq 10 applies (*53*):

$$\frac{I_A}{I_{A(X,Y)}} = 1 + \frac{X}{K_X} + \frac{Y}{K_Y}\left(1 + \frac{X}{K_X}\right) \quad (10)$$

REFERENCES

1. Amano, T., Richelson, E., and Nirenberg, M. G. (1972) *Proc. Natl. Acad. Sci. U.S.A. 69*, 258−263.

2. U.S. Congress, Office of Technology Assessment (1993) *Biological Components of Substance Abuse and Addiction*, OTA-BP-BBS-117, U.S. Government Printing Office, Washington, DC.
3. Beasley, C. M., Masica, D. N., and Potuin, J. H. (1992) *Psychopharmacology 107*, 1−10.
4. Derkach, V., Suprenant, A., and North, R. A. (1989) *Nature 339*, 706−709.
5. Maricq, A. V., Peterson, A. S., Brake, A. J., Myers, R. M., and Julius, D. (1991) *Science 254*, 432−437.
6. Yakel, J. L., Shao, X. M., and Jackson, M. B. (1991) *J. Physiol. (London) 436*, 293−308.
7. Yakel, J. L. (1996) *Behav. Brain Res. 73*, 269−272.
8. Fan, P., Oz, M., Zhang, L., and Weight, F. F. (1995) *Brain Res. 673*, 181−184.
9. Fan, P. (1994) *Neurosci. Lett. 173*, 210−212.
10. Krishtal, O. A., and Pidoplichko, V. I. (1980) *Neuroscience 5*, 2325−2327.
11. Udgaonkar, J. B., and Hess, G. P. (1987) *Proc. Natl. Acad. Sci. U.S.A. 84*, 8758−8762.
12. Hamill, O. P., Marty, A., Neher, E., Sakmann, B., and Sigworth, F. J. (1981) *Pfluegers Arch. 391*, 85−100.
13. Hess, G. P., Udgaonkar, J. B., and Olbricht, W. L. (1987) *Annu. Rev. Biophys. Chem. 16*, 507−534.
14. Neijt, H. C., Plomb, J. J., and Vijverberg, H. P. M. (1989) *J. Physiol. (London) 411*, 257−269.
15. Katz, B., and Thesleff, S. (1957) *J. Physiol. (London) 138*, 68−80.
16. Hess, G. P., Cash, D. J., and Aoshima, H. (1979) *Nature 282*, 507−534.
17. Cash, D. J., and Hess, G. P. (1980) *Proc. Natl. Acad. Sci. U.S.A. 77*, 842−846.
18. Matsubara, N., Billington, A. P., and Hess, G. P. (1992) *Biochemistry 31*, 5507−5514.
19. Geetha, N., and Hess, G. P. (1992) *Biochemistry 31*, 5488−5499.
20. Walstrom, K. M., and Hess, G. P. (1994) *Biochemistry 33*, 7718−7730.
21. Niu, L., and Hess, G. P. (1993) *Biochemistry 32*, 3831−3835.
22. Niu, L., Abood, L. G., and Hess, G. P. (1995) *Proc. Natl. Acad. Sci. U.S.A. 92*, 12008−12012.
23. Cash, D. J., and Subbarao, K. (1987) *Biochemistry 26*, 7556−7562.
24. Grewer, C., Niu, L., and Hess, G. P. (1998) *Biochemistry 38*, 7837−7846.
25. Cash, D. J., Aoshima, H., and Hess, G. P. (1981) *Proc. Natl. Acad. Sci. U.S.A. 78*, 3318−3322.
26. Huganir, R. L., Delcour, A. H., Greengard, P., and Hess, G. P. (1986) *Nature 321*, 774−776.
27. Yakel, J. L., and Jackson, M. B. (1988) *Neuron 1*, 615−621.
28. van Hooft, J. A., and Vijverberg, H. P. M. (1995) *Recept. Channels 3*, 7−12.
29. van Hooft, J. A., Kooyman, A. R., Verkerk, A., van Kleef, R. G. D. M., and Vijverberg, H. P. M. (1994) *Biochem. Biophys. Res. Commun. 199*, 227−233.
30. Woolverton, W. L., and Johnson, K. M. (1992) *Trends Pharmacol. Sci. 13*, 193−200.
31. Fuller, R. W. (1992) *Adv. Biosci. 85*, 255−271.
32. Schmidt, A. W., and Peroutka, S. J. (1989) *Eur. J. Pharmacol. 163*, 397−398.
33. Hoyer, D., Gozlan, H., Bolanos, F., Schechter, L. E., and Hamon, M. (1989) *Eur. J. Pharmacol. 171*, 137−139.
34. Jarvik, M. E., and Schneider, N. G. (1992) in *Substance Abuse: A Comprehensive Textbook* (Lowinson, J. H., Ruiz, P., and Millman, R. B., Eds., Langrod, J. G., Assoc. Ed.) pp 334−356, Williams and Wilkins, Baltimore, MD.
35. Jarvik, M. E., and Schneider, N. G. (1992) in *Substance Abuse: A Comprehensive Textbook* (Lowinson, J. H., Ruiz, P., and Millman, R. B., Eds., Langrod, J. G., Assoc. Ed.) pp 205−221, Williams and Wilkins, Baltimore, MD.
36. Betz, H. (1990) *Neuron 5*, 383−392.
37. Stroud, R. M., McCarthy, M. P., and Shuster, M. (1990) *Biochemistry 29*, 11090−11023.
38. Le Novere, N., and Changeux, J.-P. (1995) *J. Mol. Evol. 40*, 155−172.
39. Garcia-Colunga, J., and Miledi, R. (1995) *Proc. Natl. Acad. Sci. U.S.A. 92*, 2919−2923.
40. Eiselé, J.-L., Bertrand, S., Galzi, J.-L., Devillers-Thiéry, A., Changeux, J.-P., and Bertrand, D. (1993) *Nature 366*, 479−483.
41. Aoshima, H. (1990) *J. Biochem. 108*, 947−953.
42. Grant, K. A. (1995) *Drug Alcohol Depend. 38*, 155−171.
43. Neijt, H. C., Vijverberg, H. P. M., and van den Bercken, J. (1986) *Eur. J. Pharmacol. 127*, 271−274.
44. Barker, E. L., and Blakely, R. D. (1995) in *Psychopharmacology: The Fourth Generation of Progress* (Bloom, F. E., and Kupfer, D. J., Eds.) pp 321−333, Raven Press, New York.
45. Lesch, K. P., Bengel, D., Heils, A., Sabol, S. Z., Greenberg, B. D., Petri, S., Benjamin, J., Mueller, C. R., Hamer, D. H., and Murphy, D. L. (1996) *Science 274*, 1527−1531.
46. Hardman, J. G., Gilman, A. G., and Limbird, L. E., Eds. (1995) *Goodman* and *Gilman's The Pharmacological Basis of Therapeutics*, 9th ed., McGraw-Hill, New York.
47. Milburn, T., Matsubara, N., Billington, A. P., Udgaonkar, J. B., Walker, J. J., Carpenter, B. K., Webb, W. W., Marque, J., Denk, W., McCray, J. A., and Hess, G. P. (1989) *Biochemistry 28*, 49−55.
48. Hess, G. P., and Grewer, C. (1998) *Methods Enzymol. 291*, 443−473.
49. Gee, K., Carpenter, B. K., and Hess, G. P. (1998) *Methods Enzymol. 291*, 30−50.
50. Breitinger, H.-G. A., Wieboldt, R., Ramesh, D., Carpenter, B. K., and Hess, G. P. (2000) *Biochemistry 39*, 5500−5508.
51. Walker, J. W., McNamee, M. G., Pasquale, E. B., Cash, D. J., and Hess, G. P. (1981) *Biochem. Biophys. Res. Commun. 100*, 86−90.
52. Shiono, S., Takeyasu, K., Udgaonkar, J. B., Delcour, A. H., Fujita, N., and Hess, G. P. (1984) *Biochemistry 23*, 6889−6893.
53. Karpen, J. W., and Hess, G. P. (1986) *Biochemistry 25*, 1777−1785.

BI0106890